Statistical mechanics of Hénon-Heiles oscillators

V. L. Berdichevsky and M. v. Alberti
School of Aerospace Engineering, Georgia Institute of Technology, Atlanta, Georgia 30332-0150
(Received 13 December 1990; revised manuscript received 7 March 1991)

It is shown that the laws of equilibrium statistical mechanics modified for finite number of degrees of freedom are approximately valid for chaotic vibrations of the Hénon-Heiles oscillators.

I. INTRODUCTION

Statistical mechanics is an asymptotic theory valid in the limit of an infinite number of degrees of freedom. The study of small-dimensional chaos, starting from the papers by Lorenz [1] and Hénon and Heiles [2], raises the question: What is essential for the laws of statistical mechanics to be true—a large number of degrees of freedom or chaos? For ergodic Hamiltonian systems the answer was given in Ref. [3]: ergodicity (chaos) provides the validity of the laws of equilibrium thermodynamics and statistical mechanics, which ought to be slightly modified for finite numbers of degrees of freedom. Unfortunately, most small-dimensional Hamiltonian systems encountered in physics are not ergodic. Nevertheless, it seems plausible that statistical mechanics could be applied to describe systems of such kinds if the motion is "chaotic enough." Our aim is to test this hypothesis for the case of the Hénon-Heiles oscillators. We show that the motion of the Hénon-Heiles oscillators matches very accurately the predictions of small-dimensional statistical mechanics for high-energy vibrations and we also study the changes that occur when the energy level decreases. First we outline, according to Ref. [3], thermodynamics and statistical mechanics of finite-dimensional ergodic Hamiltonian systems.

II. EQUILIBRIUM THERMODYNAMICS AND STATISTICAL MECHANICS OF ERGODIC HAMILTONIAN SYSTEMS

Consider a Hamiltonian system with generalized coordinates $q=(q_1,\ldots,q_n)$, generalized momenta $p=(p_1,\ldots,p_n)$, and the Hamilton function H, which depends also on some parameters $y=(y_1,\ldots,y_k)$, describing the influence of external factors. The Hamilton equations are

$$\dot{p}=-\frac{\partial H(p,q,y)}{\partial q},\quad \dot{q}=\frac{\partial H(p,q,y)}{\partial p}\ . \tag{2.1}$$

If the parameters y are fixed, trajectories of the system belong to energy surfaces $H(p,q,y)=E=\text{const}$. It is assumed that the system is ergodic on energy surfaces and every energy surface bounds a finite volume of the phase space $\Gamma(E,y)$.

The following three statements express the laws of equilibrium thermodynamics and statistical mechanics.

A. Temperature

Denote by $\langle\cdot\rangle$ the averaging operator along a trajectory. For any function $g(p,q)$ the quantity $\langle g\rangle$ does not depend on the trajectory chosen on an energy surface (up to some exceptional sets with zero measure). For any ergodic Hamiltonian system the equipartition law is valid:

$$\left\langle p_1\frac{\partial H}{\partial p_1}\right\rangle=\left\langle p_2\frac{\partial H}{\partial p_2}\right\rangle=\cdots=\left\langle p_n\frac{\partial H}{\partial p_n}\right\rangle\ . \tag{2.2}$$

The common value of (2.2) is called by definition the absolute temperature T. This temperature is expressed in terms of the function $\Gamma(E,y)$ by the relation

$$T=\frac{\Gamma(E,y)}{\partial\Gamma(E,y)/\partial E}\ . \tag{2.3}$$

B. Entropy

Allow slow variations of the external parameters y. Then the energy of the system is also changed. The quantity $\Gamma(E,y)$ is an adiabatic invariant, i.e., could be considered as a constant (in some sense) in the course of the variation in E,y (the Hertz-Kasuge theorem [4,5]). Any adiabatic invariant is a function of $\Gamma(E,y)$ (Kasuge's theorem [5]). It is natural to introduce the entropy of a finite-dimensional system in such a way that (1) entropy is an adiabatic invariant; (2) the energy equation is true, $dE=dA+TdS$, where dA is the work done by external forces in order to change the parameters y.

For Hamiltonian systems the work done by external forces is

$$dA=\left\langle\frac{\partial H}{\partial t}\right\rangle dt=\left\langle\frac{\partial H}{\partial y_i}\right\rangle dy_i\ .$$

The mean value $\langle\partial H/\partial y_i\rangle$ is calculated for the ergodic system in terms of the function $\Gamma(E,y)$:

$$dA=-\frac{1}{\partial\Gamma(E,y)/\partial E}\frac{\partial\Gamma(E,y)}{\partial y_i}dy_i\ .$$

Hence, the energy equation takes the form

$$dE=-\frac{1}{\partial\Gamma/\partial E}\frac{\partial\Gamma}{\partial y_i}dy_i+TdS\ . \tag{2.4}$$

It is easy to find that the only quantity satisfying the requirements (1) and (2) and Eq. (2.4) is

$$S(E,y)=\ln\Gamma(E,y)+\text{const}. \tag{2.5}$$

This function $S(E,y)$ is linked with the temperature T by the relation

$$\frac{1}{T}=\frac{\partial S(E,y)}{\partial E} . \tag{2.6}$$

The work of external forces is found in terms of entropy as

$$dA=-T\frac{\partial S(E,y)}{\partial y_i}dy_i . \tag{2.7}$$

Note that usually in statistical mechanics, entropy is introduced by another formula,

$$S=\ln\frac{\partial\Gamma}{\partial E}+\text{const.} \tag{2.8}$$

The quantities (2.5) and (2.8) coincide in the limit $n\to\infty$, and it does not matter which of the two formulas (2.5) and (2.8) is used to calculate the entropy. Both expressions were known to Gibbs [6]. Historically, the quantity (2.8) got preference. However, for finite n the quantities (2.5) and (2.8) are essentially different. Unlike the entropy (2.5), the quantity (2.8) is not an adiabatic invariant and does not satisfy the energy equation (2.4).

C. Entropy and probability

Consider some set of characteristics $\Phi_1(q,p),\ldots,\Phi_m(q,p)$ and denote by $f(z_1,\ldots,z_m)$ the probability density function of these characteristics. The probability density function $f(z_1,\ldots,z_m)$ can be expressed in terms of the entropy $S(E,z)$ of some auxiliary Hamiltonian system. This system is obtained from the original one by setting the kinematic constraints $\Phi_1(q,p)=z_1,\ldots,\Phi_m(q,p)=z_m$. The relation between $f(z)$ and $S(E,z)$ has the form (we do not mention here explicitly the dependence on the external parameters y)

$$f(z)=\frac{1}{\partial\Gamma(E)/\partial E}\frac{\partial}{\partial E}e^{S(E,z)} . \tag{2.9}$$

The formula (2.9), derived in Ref. [3], is an exact relation valid for finite fluctuations of characteristics. It generalizes the Einstein formula

$$f(z)=\text{const}\,e^{S(E,z)} \tag{2.10}$$

derived for small fluctuations near equilibrium state: (2.9) reduces to (2.10) in the limit $n\to\infty$.

Note that the Gibbs distribution $f(x)=Z^{-1}\exp[-\beta H(x)]$ can be derived from the Einstein formula (2.10); therefore, the Einstein formula could be considered as the basic relation of equilibrium statistical mechanics. Formula (2.9) plays the analogous role in statistical mechanics of systems with finite numbers of degrees of freedom.

III. THE HÉNON-HEILES OSCILLATORS

One of the first examples of chaotic motion of small-dimensional system was discovered by Hénon and Heiles in 1964 [2]. They considered a system of two interacting oscillators. The first oscillator is simply a harmonic oscillator with the Hamilton function $H_1=(p_1^2+q_1^2)/2$. The second oscillator is a nonlinear oscillator with the following properties: (1) it has a stable equilibrium point at $q_2=0$; (2) the frequency of linear vibrations in the vicinity of this equilibrium point is equal to the frequency of the first oscillator; (3) if q_2 exceeds some value, the oscillator tends to escape the origin. The potential energy $U_2(q_2)$ was chosen as

$$U_2(q_2)=\tfrac{1}{2}q_2^2-\tfrac{1}{3}q_2^3 .$$

Of course, this is an approximation of the situation when the second oscillator has two stable points and one studies the vibration in the vicinity of one of them.

Hénon and Heiles introduced an asymmetric interaction of the form $H_{12}=q_1^2q_2$, so the total Hamilton function is

$$\begin{aligned} H&=\tfrac{1}{2}(p_1^2+p_2^2)+U(q_1,q_2) ,\\ U(q_1,q_2)&=\tfrac{1}{2}q_1^2+U_2(q_2)+q_1^2q_2 . \end{aligned} \tag{3.1}$$

This system has one stable equilibrium point at the origin: $q_1=q_2=0$, and three unstable equilibrium points $P_1(q_1=0,\ q_2=1)$, $P_2(3^{1/2}/2,-\frac{1}{2})$, $P_3(-3^{1/2}/2,-\frac{1}{2})$. They are shown in the contour plot of the potential energy $U(q_1,q_2)$ (Fig. 1). The separatrices connecting the unstable points are straight lines. These separatrices correspond to an energy level $U=\frac{1}{6}$. All contour lines with energy levels less than $\frac{1}{6}$ lie inside the triangle $P_1P_2P_3$.

For the following references we give here the Poincaré sections $p_1=q_1=0$ of energy surfaces with $E=\frac{1}{6}$ (Fig. 2)

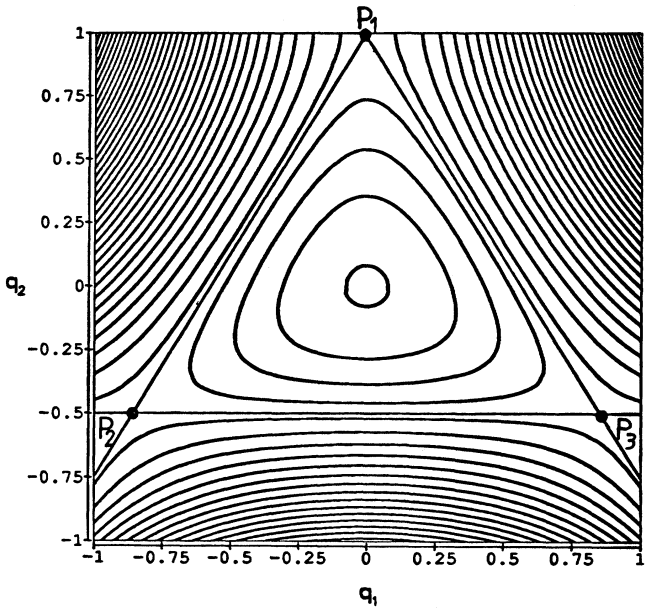

FIG. 1. Equipotential lines of the potential function. The points P_1, P_2, and P_3 are unstable equilibrium points of the system. The origin ($q_1=q_2=0$) is a stable equilibrium point. The particular energy $E=\frac{1}{6}$ represents the maximum energy, for which the motion is bounded.

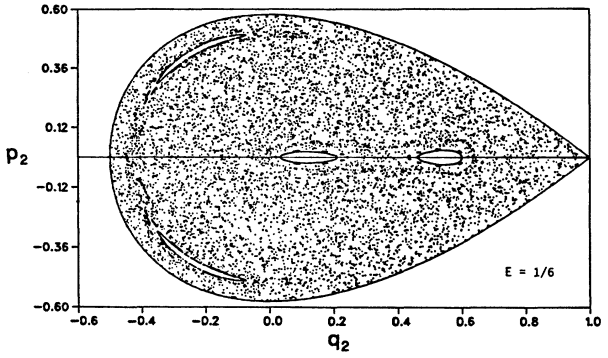

FIG. 2. Poincaré section ($q_1=0$, $p_1>0$) for an energy level $E=\frac{1}{6}$. Poincaré sections are obtained by computing the system's trajectory and plotting the successive intersections of the trajectory with the q_1 plane in the upward direction ($p_1>0$). Smooth curves indicate ordered motion, while scattered points indicate chaotic motion.

and $E=\frac{1}{8}$ (Fig. 3). It can be observed that the motion is almost completely chaotic for the highest energy $E=\frac{1}{6}$: periodic orbits occupy a small part of the energy surface. The portion of ordered motion increases as the energy level decreases. Figures 2 and 3 show that the Hénon-Heiles system is not an ergodic Hamiltonian system, because the set of periodic orbits has a nonzero measure. Nevertheless, we shall treat this system as approximately ergodic and predict probability characteristics and thermodynamic functions.

The key quantity is the volume of phase space $\Gamma(E)$, bounded by the energy surface $H(p_1,p_2,q_1,q_2)=E$. This volume can be expressed in terms of the area $A(e)$ of the region in the (q_1,q_2) plane, bounded by the curve $U(q_1,q_2)=e$. Really, one can write

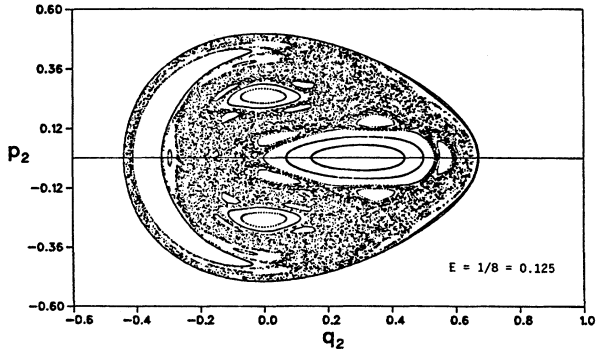

FIG. 3. Poincaré section ($q_1=0$, $p_1>0$) for an energy level $E=\frac{1}{8}$. Figures 2 and 3 show that the portion of phase space occupied by chaotic motion decreases with the total energy of the system. For the maximum energy $E=\frac{1}{6}$ the motion is almost completely chaotic, while for $E=\frac{1}{8}$ a large part of the phase space is covered by ordered motion.

$$\Gamma(E)=\int_{H(p_1,p_2,q_1,q_2)\le E} dp_1dp_2dq_1dq_2$$
$$=\int\left[\int_{p_1^2+p_2^2/2\le E-U(q_1,q_2)} dp_1dp_2\right]dq_1dq_2$$
$$=2\pi\int[E-U(q_1,q_2)]dq_1dq_2 .$$

This last integral is extended over the region of positiveness of the integrand. It can be rewritten as follows:

$$\Gamma(E)=2\pi\int_0^E(E-e)dA(e) .$$

After integrating by parts we have

$$\Gamma(E)=2\pi\int_0^E A(e)de . \tag{3.2}$$

Hence

$$\frac{d\Gamma}{dE}=2\pi A(E) . \tag{3.3}$$

From (2.5) and (2.6) we obtain the following expressions for entropy and temperature of the Hénon-Heiles oscillators:

$$S(E)=\ln\int_0^E A(e)de+\text{const} ,$$
$$T(E)=\frac{1}{A(E)}\int_0^E A(e)de . \tag{3.4}$$

The area $A(e)$ can be calculated using the expression

$$A(e)=2\int_a^b\left[\frac{2[e-U_2(x)]}{1+2x}\right]^{1/2}dx , \tag{3.5}$$

where a and b are the two smallest roots of the cubic equation $U_2(x)=e$ (assume $a\le b$). The integral in (3.5) could be reduced to the standard elliptic integrals. However, we prefer to find this and similar integrals encountered below numerically. The dependence of A on e is shown in Fig. 4.

Besides temperature, we shall study probability density functions of the coordinate and momentum of each oscillator and denote them by $f_1(p,q)$ and $f_2(p,q)$, respectively. Consider first the probability density function of the

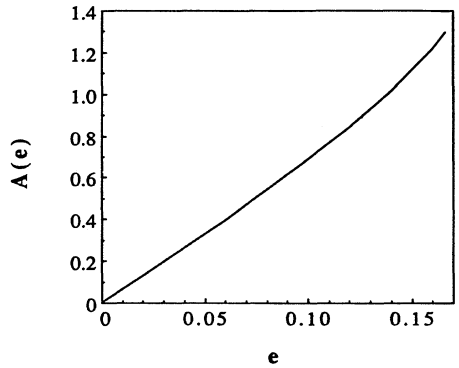

FIG. 4. Area $A(e)$ of the region in the (q_1,q_2) plane bounded by the curve $U(q_1,q_2)=e$ vs e.

second oscillator $f_2(p,q)$. This probability density function is equal to zero outside the region of possible values of p_2,q_2, i.e., the set of all points in the (p_2,q_2) plane that could be visited by trajectories of the system. Denote this region by R_2. In accordance with the ergodic hypothesis, it is analytically defined as the set of such points (p_2,q_2) that for some values of p_1,q_1 the equality $H(p_1,p_2,q_1,q_2)=E$ is satisfied. In order to describe R_2 explicitly, it is convenient to introduce the function

$$h_2(p_2,q_2)=\min_{p_1,q_1} H(p_1,q_1,p_2,q_2) \ . \tag{3.6}$$

The region R_2 is extracted by the inequality

$$h_2(p_2,q_2)\le E \ . \tag{3.7}$$

The function $h_2(p_2,q_2)$ is obviously equal to the energy of the second oscillator

$$h_2(p_2,q_2)=\tfrac{1}{2}p_2^2+U_2(q_2) \ ,$$

and the admissible regions coincide with the interiors of energy levels of the second oscillator in its free vibrations.

Following the general scheme, in order to find f_2 one has to calculate the entropy of the system with the kinematic constraints $p_2=p$, $q_2=q$. Trajectories $p_1(t)$ and $q_1(t)$ of the constrained system lie on the curve

$$\tfrac{1}{2}(p_1^2+q_1^2)+q_1^2q_2=E-\tfrac{1}{2}p_2^2-U_2(q_2) \ . \tag{3.8}$$

The curve (3.8) is an ellipse with the half axes

$$\{2[E-\tfrac{1}{2}p_2^2-U_2(q_2)]\}^{1/2}$$

and

$$\{2[E-\tfrac{1}{2}p_2^2-U_2(q_2)]/(1+2q_2)\}^{1/2} \ .$$

The area $\Gamma_2(E,p_2,q_2)$ bounded by this ellipse is

$$\Gamma_2(E,q_2,p_2)=2\pi[E-\tfrac{1}{2}p_2^2-U_2(q_2)]/\sqrt{1+2q_2} \ .$$

Hence, the entropy of the constrained system is

$$S_2(E,q_2,p_2)=\ln\frac{E-\frac{1}{2}p_2^2-U_2(q_2)}{\sqrt{1+2q_2}}+\text{const.} \tag{3.9}$$

From (2.9) and (3.3) we find the probability density function of the coordinate and momentum of the second oscillator:

$$f_2(E,q_2,p_2)=\frac{1}{A(E)\sqrt{1+2q_2}} \ . \tag{3.10}$$

Note a remarkable peculiarity of this function: It does not depend on the momentum.

Similarly, one can find the probability density function of the first oscillator. The domain of this function is

$$h_1(p_1,q_1)\le E \ ,$$

where

$$h_1(p_1,q_1)=\tfrac{1}{2}p_1^2+q_1^2-\tfrac{2}{3}(\tfrac{1}{4}+q_1^2)^{3/2}+\tfrac{1}{12} \ . \tag{3.11}$$

The trajectories of the constrained system lie on the curve in the (p_2,q_2) plane:

$$\tfrac{1}{2}p_2^2+\tfrac{1}{2}q_2^2-\tfrac{1}{3}q_2^3+q_1^2q_2=E-\tfrac{1}{2}(p_1^2+q_1^2) \ .$$

It bounds the region with the area $\Gamma_1(E,p_1,q_1)$ equal to

$$\begin{aligned}\Gamma_1(E,p_1,q_1)&-2\int_a^b p_2\,dq_2\\ &=2\sqrt{2}\int_a^b\{[E-\tfrac{1}{2}(p_1^2+q_1^2)]\\ &\qquad-\tfrac{1}{2}q_2^2+\tfrac{1}{3}q_2^3-q_1^2q_2\}^{1/2}dq_2\end{aligned} \tag{3.12}$$

where a and b are the two smallest zeros of the integrand. In accordance with (2.5), $S_1(E,p_1,q_1)=\ln\Gamma_1$, and

$$f_1(p_1,q_1)=\frac{1}{2\pi A(E)}\frac{\partial\Gamma_1}{\partial E} \ .$$

Since the integrand is zero on the bounds, the differentiation with respect to the energy can be interchanged with the integration, thus

$$\begin{aligned}f_1(p_1,q_1)=&\frac{1}{2\pi A(E)}\sqrt{2}\\ &\times\int_a^b\{E-\tfrac{1}{2}(p_1^2+q_1^2)]-\tfrac{1}{2}x^2\\ &\qquad+\tfrac{1}{3}x^3-q_1^2x\}^{-1/2}dx \ .\end{aligned} \tag{3.13}$$

This integral has been found pointwise by a numerical procedure. Now we proceed to the comparison of the theoretical relations (2.3), (2.5), and (2.9) with numerical results.

IV. TEMPERATURE

The first important question is: how strongly do the islands of ordered motion affect the equipartition law? We calculated the "temperatures" of the oscillators:

$$T_1=\frac{1}{\Theta}\int_0^\Theta p_1^2dt, \quad T_2=\frac{1}{\Theta}\int_0^\Theta p_2^2dt \tag{4.1}$$

for various energy levels and starting points. The averaging time Θ was chosen between approximately 10^3 and 10^5 periods of vibrations of the first oscillator, according to the rate of the convergence that was observed. Figure 5 shows the dependence of T_1 and T_2 on the averaging

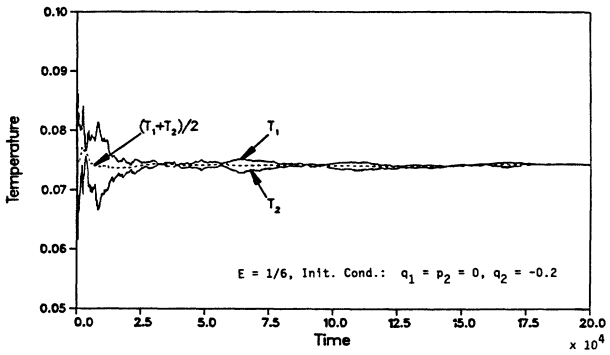

FIG. 5. Numerical temperatures T_1 and T_2 [according to (4.1)] vs time.

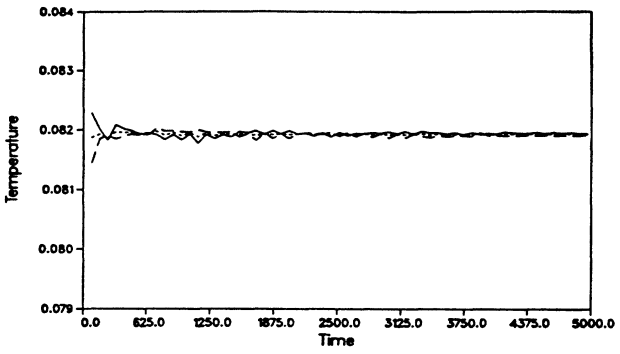

FIG. 6. Temperatue vs time for $E=\frac{1}{6}$ and initial conditions $q_2=0.02, p_2=0$.

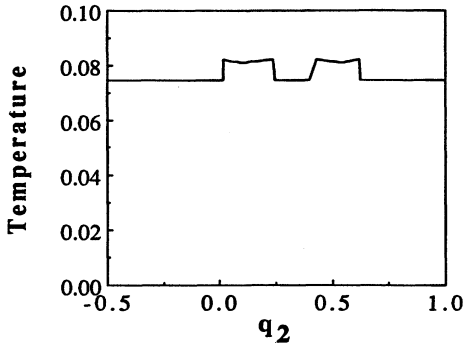

FIG. 8. Temperature profile along the q_2 axis ($p_2=0$), $E=\frac{1}{6}$.

time Θ for a chaotic trajectory and the maximum energy $E=\frac{1}{6}$. It can be clearly seen that T_1 and T_2 converge to a common value $T=(T_1+T_2)/2\cong 0.074\,33$. The error $|T_1-T_2|/T$ is below 0.1%. All calculations for chaotic trajectories on this energy level yield the same result. This supports the validity of the equipartition law for the highest energy level.

The temperature on trajectories of ordered motion show the same behavior; only the rate of convergence is much faster. (One might assume that it occurs because of the smaller dimensionality of a torus compared with that of the energy surface.)

Figure 6 shows a run for $E=\frac{1}{6}$ and initial point $q_2=0.02, p_2=0$ on the island. The temperatures T_1 and T_2 converge quite quickly towards $T\cong 0.0819$, the corresponding error being $\Delta T=0.0003$ or 0.04%. The picture is a little different for trajectories belonging to the left island in Fig. 2. Here, as shown in Fig. 7, the temperatures T_1 and T_2 stabilize clearly but they do not converge towards exactly the same value. However, the difference between T_1 and T_2 is rather small: $\Delta T=0.0007$ or 0.9%.

Figure 8 shows a profile of the mean temperature T along the q_2 axis ($p_2=0$) for the maximum energy $E=\frac{1}{6}$. It can be seen that the temperature on the islands of ordered motion is slightly higher than the temperature of the chaotic sea.

Similar experiments for lower energy levels show the same type of behavior as observed for the maximum energy $E=\frac{1}{6}$. Figure 9 shows the mean temperature T of chaotic trajectories as well as the theoretical temperature T calculated according to (3.4) versus the energy level E. The correlation between the numerical and the theoretical curves is very good. The largest margin of error is about 3%.

An unexpected result of these experiments is that the equipartition law is valid even for moderate and low energy levels on both chaotic and ordered trajectories, although in these cases the fraction of the phase space that is occupied by islands of ordered motion is quite large and the assumption of ergodicity is strongly violated. In order to eliminate the possible resonance effects that could occur because of the equality of the frequencies of the two oscillators in the linear region, a modification of the Hénon-Heiles system of the form

$$H=\tfrac{1}{2}p_1^2+\tfrac{1}{2}ap_2^2+\tfrac{1}{2}q_1^2+U_2(q_2)+q_1^2q_2$$

was tested for different values of the distortion parameter

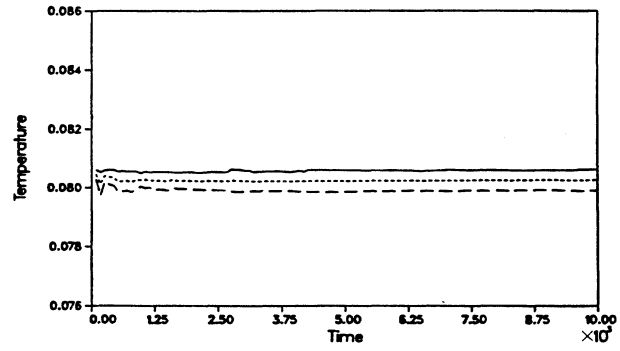

FIG. 7. Temperature vs time for $E=\frac{1}{6}$ and initial conditions $q_2=-0.2, p_2=0.45$.

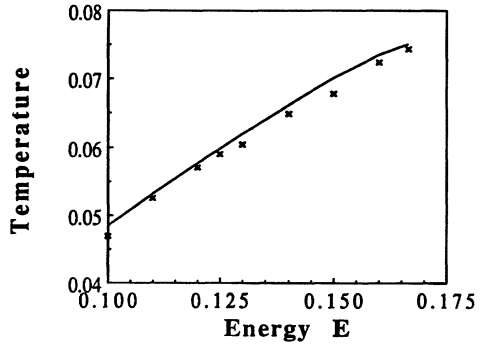

FIG. 9. Temperature as a function of the energy E. Solid line represents T from Eq. (3.4); the crosses, numerical T.

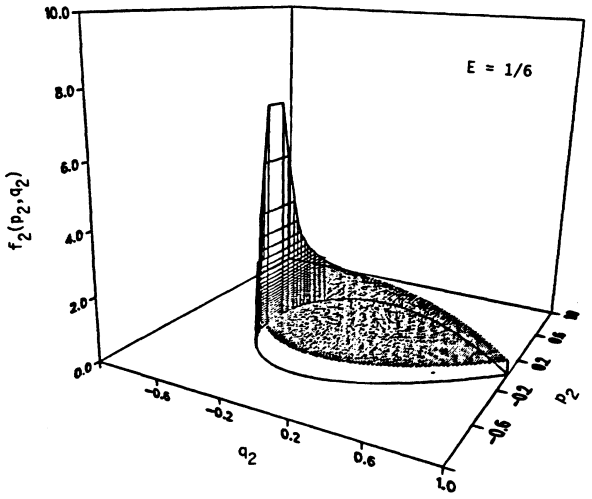

FIG. 10. Three-dimensional graph of the probability density function f_2 [according to (3.10)]. The curve on the bottom is the boundary of the domain on which f_2 is defined (compare with the boundary in Fig. 2).

a (such as $a=1.5$ or 2.5) that result in nonresonance cases. The results are as follows: for chaotic trajectories, the equipartition law is valid with approximately the same accuracy as for the Hénon-Heiles oscillators, provided that the size of the region of ordered motion is small compared to the chaotic one. The temperatures of trajectories on islands of ordered motion can differ essentially (up to 90%), no matter how big these islands are.

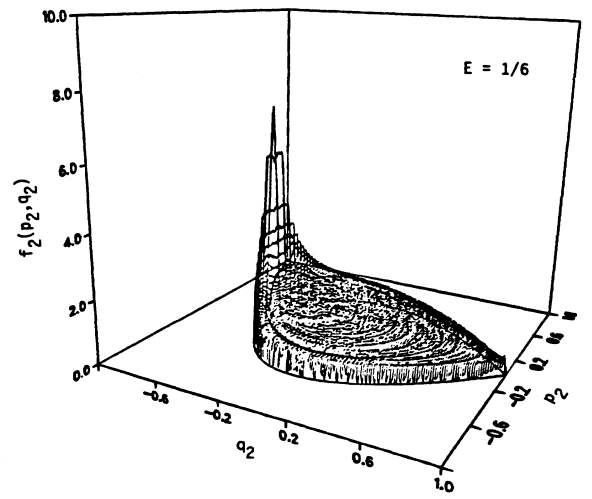

FIG. 11. Three-dimensional graph of the probability density function f_2 (numerical). This probability density function was determined by a bin-counting experiment. The observation time was $t=10^6$ or about 160 000 periods with a total number of $N=25\times10^6$ position measurements. The reason that the probability density seems to drop on the boundary is that bins on this boundary were treated just like regular bins, although they are smaller.

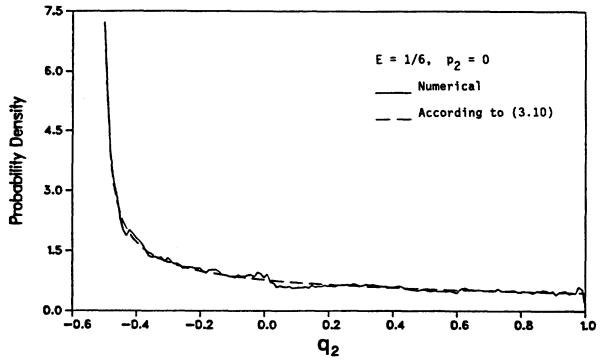

FIG. 12. Two-dimensional slice of the probability density function f_2. The small fluctuations will presumably level out for longer observation times. However, there are some dents, like the one between $q_2=0$ and $q_2=0.2$, that are caused by islands of ordered motion (compare with Fig. 2). This phenomenon can be observed more clearly in Figs. 11 and 12.

That led us to the conclusion that the validity of the equipartition law in the case of moderate energy vibrations for the Hénon-Heiles oscillators is due to their resonant frequencies.

V. PROBABILITY DENSITY FUNCTIONS

A numerical probability density function was obtained by a simple bin-counting experiment, during which the trajectory of the system is calculated for a very long time interval and the current coordinate position of the trajectory is noted at every step of the integration. The probability of the event that the trajectory of the system is within an area element A of its phase space is determined by the fraction formed by the number of times the trajectory was observed to be within A divided by the total number of observations. Figure 10 shows the probability density function f_2 according to (3.10) for $E=\frac{1}{6}$, while Fig. 11 depicts its numerical counterpart. In order to compare the theoretical and numerical results, two-

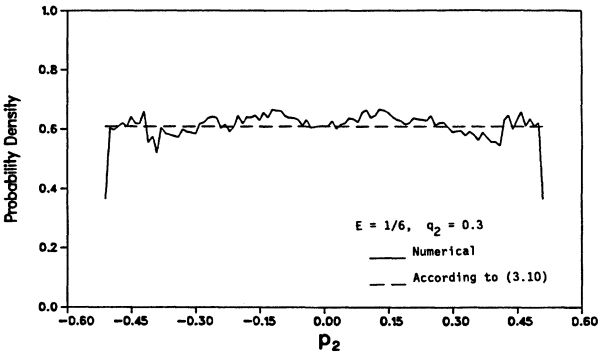

FIG. 13. Two-dimensional slice of the probability density function f_2.

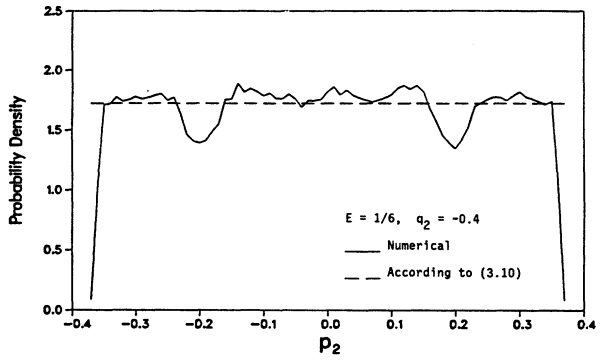

FIG. 14. Two-dimensional slice of the probability density function f_2.

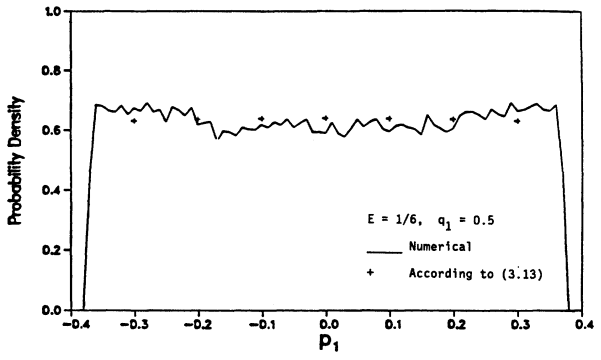

FIG. 16. Two-dimensional slice of the probability density function f_1.

dimensional slices of the probability density functions for specific q or p were extracted out of the data; some of them are shown in Figs. 12 and 13. Figure 12 shows the probability density functions f_2 versus q_2 at $p_2=0$. The shape of the theoretical curve is matched very nicely and the maximal error is below 3%. Figures 13 and 14 show similar slices for a constant $q_2=0.3$ and $q_2=-0.4$, respectively. In accordance with (3.10), the probability density function f_2 does not depend on p_2 (dashed line). The real probability density function obeys this property well enough at all points except at the two dents in Fig. 14. It can be seen from Fig. 2 that they are caused by islands of ordered motion. In fact, it has been observed that all deviations between numerical and theoretical probability density functions f_2 are due to islands of ordered motion (except some small numerical fluctuations, which will presumably level out for longer experiments).

The analogous results for the probability density function of the first oscillator are shown in Figs. 15 and 16. For lower energies, these deviations are larger; as seen in Fig. 17 ($E=\frac{1}{8}$, $p_2=0$) and Fig. 18 ($E=\frac{1}{8}$, $q_2=0$), for a moderate energy $E=\frac{1}{8}$ the error can be as large as 45%. It is interesting that the theoretical curve is located with respect to the real one in such a way as to give close

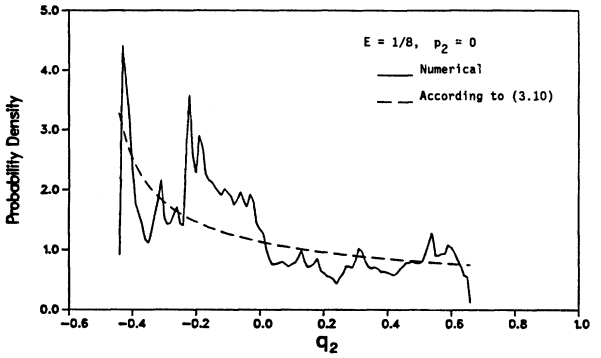

FIG. 17. Two-dimensional slice of the probability density function f_2.

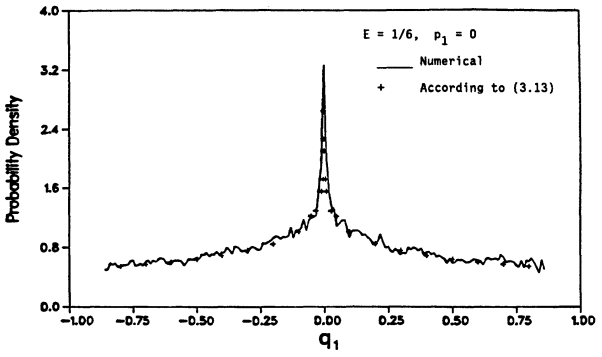

FIG. 15. Two-dimensional slice of the probability density function f_1.

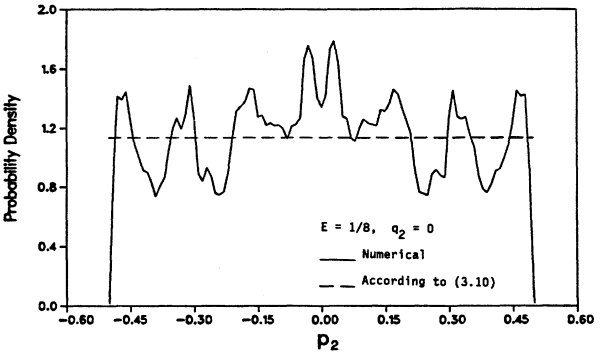

FIG. 18. Two-dimensional slice of the probability density function f_2.

momentum characteristics. In particular, the differences in temperature do not exceed 3%.

VI. CONCLUSIONS

The considerations above show that statistical mechanics of finite-dimensional systems predicts quite accurately the probabilistic and thermodynamic characteristics of the chaotic motion of the Hénon-Heiles oscillators. All numerical aspects of this study are generalizable to other Hamiltonian systems with the number of degrees of freedom larger than 2. One can expect that statistical mechanics of finite-dimensional systems could be a reasonable tool for the description of developed chaos in small-dimensional Hamiltonian systems. We would like to call attention to the two interesting open problems here: the extension of the theory on nondeveloped chaos, where one could expect the appearance of a number of temperatures and entropies, and on systems with dissipation.

ACKNOWLEDGMENT

The authors wish to thank Dr. C. V. Smith for helpful discussions.

[1] E. N. Lorenz, J. Atmos. Sci. **20**, 130 (1963).
[2] M. Henon and C. Heiles, Astron. J. **69**, 73 (1964).
[3] V. Berdichevsky, J. Appl. Math. Mech. **52**, 738 (1988).
[4] P. Hertz, Ann. Phys. (Leipzig) **33**, 12 (1910); **33**, 13 (1910).
[5] T. Kasuge, Proc. Jpn. Acad. **37**, 7 (1961).
[6] J. Gibbs, *Thermodynamics* (Yale University, New Haven, 1902); *Statistical Mechanics* (Yale University, New Haven, 1914).